Journal of Power Sources 232 (2013) 209–218

Contents lists available at SciVerse ScienceDirect

Journal of Power Sources

journal homepage: www.elsevier.com/locate/jpowsour

# Using probability density function to evaluate the state of health of lithium-ion batteries

Xuning Feng [a], Jianqiu Li [a], Minggao Ouyang [a,*], Languang Lu [a], Jianjun Li [b], Xiangming He [a,b]

[a] State Key Laboratory of Automotive Safety and Energy, Tsinghua University, Beijing 100084, China
[b] Institute of Nuclear and New Energy Technology, Tsinghua University, Beijing 100084, China

## HIGHLIGHTS

- A new method, named probability density function(PDF), is proposed to help evaluate the SOH of power Li-ion battery.
- We have verified that the PDF method and the existing method incremental capacity analysis(ICA) have the same essence.
- According to the experimental data, the PDF method can get similar results with that of cyclic voltammogram.
- Based on the PDF method, we propose an online algorithm to evaluate the SOH of battery using partial charging or discharging.

## ARTICLE INFO

*Article history:*
Received 5 October 2012
Received in revised form
1 January 2013
Accepted 3 January 2013
Available online 21 January 2013

*Keywords:*
Probability density function
State of health
Statistical frequency
Lithium-ion battery
Cycle life

## ABSTRACT

A new method, probability density function (PDF), is proposed for evaluating the state of health (SOH) of electric storage batteries by analyzing the charge/discharge (C/D) data. First, a comparison of the PDF method, the cyclic voltammogram (CV), incremental capacity analysis (ICA) and differential voltage analysis (DVA) is provided. The mathematical basis of the four methods are in agreement. Moreover, the PDF method and the ICA/DVA have an equivalence verified by mathematical derivation. Thus the results acquired by the PDF and the ICA/DVA are quite similar. $LiFePO_4$ and $LiMn_2O_4$ batteries are tested to demonstrate the PDF method. Coin cells are tested by the PDF and the CV methods. Results show that the PDF curves and the CV curves have similar shapes. In addition, durability tests are conducted on four commercial batteries to analyze the aging regularities using the PDF method. The PDF results show that the height of the peak reduces as the battery capacity fades. Employing the regularity of peak height reduction with battery aging, an algorithm is proposed to evaluate the SOH online. The PDF method extends the application of the ICA/DVA method. The PDF algorithm is promising to be used in the online SOH evaluation of lithium-ion batteries.



## 1. Introduction

Currently, lithium-ion batteries are favored by researchers as a promising power source for electric vehicles. $LiFePO_4$ and $LiMn_2O_4$ are two of the most popular cathode materials for lithium-ion batteries for use in electric vehicles. For a battery with cathode of $LiFePO_4$ [1] or $LiMn_2O_4$ [2], voltage plateaus can be observed within their working ranges. To analyze the chemical reactions within the cell, the cyclic voltammogram (CV) is employed [3,4]. The locations of the CV peaks indicate the corresponding chemical reactions [3,4]. The CV has been used in previous research on $LiFePO_4$ and $LiMn_2O_4$.

The state of health (SOH) of the battery reflects the degradation of the battery capacity. To perform battery management, an evaluation of the SOH is critical [5,6]. Incremental capacity analysis (ICA) is used to analyze the SOH by differentiation of the voltage and the capacity [5,7]. Differential voltage analysis (DVA) is used to analyze the battery charge/discharge (C/D) data by employing the inverse data of the ICA [5,8,9]. Commonly, the AC impedance spectrum is also employed to evaluate the SOH of the battery [10,11]. In addition to these classic methods, the probability density function (PDF) method is also available to analyze the conditions of the battery [12].

*Abbreviations:* BMS, battery management system; C/D, charge/discharge; CV, cyclic voltammogram; DVA, differential voltage analysis; ICA, incremental capacity analysis; PDF, probability density function; SOH, state of health.

* Corresponding author. Tel.: +86 10 62773437; fax: +86 10 62785708.
*E-mail addresses:* fxn07@mails.tsinghua.edu.cn, xuning.feng@qq.com (X. Feng), ouymg@tsinghua.edu.cn (M. Ouyang).

0378-7753/$ – see front matter © 2013 Elsevier B.V. All rights reserved.
http://dx.doi.org/10.1016/j.jpowsour.2013.01.018

**Nomenclature**

| | |
|---|---|
| $C$ | charge or discharge current rate for a specific battery |
| $C_{QV}$ | an abbreviation for $dQ/dV$ |
| $dQ$ | differential capacity |
| $\delta Q$ | capacity charged or discharged in 1 s with a specific current |
| $dt$ | differential time |
| $dV$ | differential voltage |
| $\delta V$ | sampling resolution of voltage, 1 mV |
| $f$ | the function describing the relationship between $V$ and $Q$ used in incremental capacity analysis, $Q = f(V)$ |
| $f^{-1}$ | the inverse function describing the relationship between $V$ and $Q$ used in incremental capacity analysis, $V = f^{-1}(Q)$ |
| $f_{CV}$ | the function describing the relationship between current and voltage in cyclic voltammogram test |
| $f_{IC\text{-}DV}$ | the function describing the relationship between current and voltage in ICA/DVA |
| $g$ | the function describing the relationship between $dQ/dV$ and $V$ used in incremental capacity analysis, $dQ/dV = g(V)$ |
| $I$ | current |
| $k,l,m,n$ | discrete time indices |
| $L$ | the number of samples in the data set, data length |
| $N_k$ | the frequency number for $V_{d,k}$ |
| $p_k$ | the probability of $V_{d,k}$, $p_k = N_k/L$ |
| $Q$ | charged or discharged capacity in Ah |
| $Q_0$ | the initial capacity of battery charging or discharging, $Q_0 = 0$ |
| $Q_a$ | analog capacity calculated by $Q_a = f^{-1}(V_d)$ |
| $Q_{a,k}$ | analog capacity calculated by $Q_{a,k} = f^{-1}(V_{d,k})$ |
| $Q_{C0}$ | the total capacity exchanged in a charging or discharging cycle |
| $Q_d$ | integrated discrete capacity corresponding to $V_d$ |
| $Q_{d,k}$ | integrated discrete capacity corresponding to $V_{d,k}$, with time serial number k |
| $V$ | voltage |
| $V_0$ | the starting voltage in battery charging or discharging |
| $V_a$ | analog voltage |
| $V_d$ | sampled digital voltage |
| $V_{d,k}$ | sampled digital voltage, d denotes digital, k is the sample index |

This paper shows that the PDF, the CV and the ICA/DVA methods for evaluating SOH are in agreement. More importantly, verified by mathematical derivations, the PDF method and ICA/DVA have the same basis. Hence, the PDF, the CV and the ICA/DVA method produce similar results. Comparing with the CV, the ICA/DVA are more applicable because they only need analysis on C/D data. However, it is difficult to calculate a differential voltage $dV$ from the sampled data because of the voltage plateaus that are characteristic of $LiFePO_4$ and $LiMn_2O_4$. Noise peaks occur when calculating $dV$ if using the ICA/DVA [9], so curves must first be fitted to the voltage data [9]. Requirement of curve fitting obstructs the online application of the ICA/DVA. This paper demonstrates that, the PDF method can produce similar results to those of the ICA/DVA without curve fitting. Based on the PDF method, a possible statistical algorithm without curve fitting is provided for evaluating the SOH of a battery. This algorithm is more practical to be embedded in a battery management system (BMS).

## 2. Mathematical derivations

### 2.1. The relationship between CV and ICA/DVA

In this section, a derivation is provided to explain the relationship between CV and ICA/DVA.

A typical CV involves sweeping the electrode potential between limits $E_1$ and $E_2$ at a known sweep rate, $v$, and on reaching the potential $E_2$ the sweep is reversed (at the same rate), see Fig. 1 [3]. The CVs for $LiFePO_4$ and $LiMn_2O_4$ are shown in Fig. 2 [13,14]. For the CV, the curve can be described by a function:

$$I = f_{CV}(V) \tag{1}$$

Cyclic voltammetry can only be performed on a cell with specific instruments. However, at present, most storage batteries consist of many parallel cells inside a casing. So the CV can not be used to test the storage batteries. To test a battery, a common method is to charge or discharge the battery with a controlled current or a controlled voltage [15–17]. Only voltage, current and temperature are available for the BMS. And the ICA/DVA can analyze the voltage and the current data.

Consider a typical ICA/DVA process: assume that $Q$ represents the capacity in units of Ah (ampere-hours) or As (ampere-seconds). Generally, the $Q$–$V$ relation is obtained from a C/D test at a constant current. The value of $Q$ is calculated from Eq. (2), and $V$ is sampled varying with time. The relationship between $Q$ and $V$ can be described by Eq. (3).

$$Q = It \tag{2}$$

$$V = f(Q),\ Q = f^{-1}(V) \tag{3}$$

The slope $dQ/dV$ can be re-written as shown in Eq. (4), but $dQ/dV$ remains a function of $V$. In addition, it seems that the current $I$ should be a function of $V$, as shown in Eq. (5). Logically and interestingly, Eq. (1) and Eq. (5) are of the same type. Moreover, the CV and the ICA have the same shape especially for the peak positions. However, the dependent variable for the CV is the current $I$, whereas the dependent variable of the ICA is a composite of $I$ and $dV/dt$. And $dV/dt$ is not constant in incremental capacity analysis. The mathematical derivation is similar for the DVA. However, the ICA and the DVA provide a more practical method for the SOH evaluation of the battery than the CV.

$$\left(f^{-1}\right)' = \frac{\mathrm{d}Q}{\mathrm{d}V} = \frac{\mathrm{d}(It)}{\mathrm{d}V} = \frac{I\mathrm{d}t}{\mathrm{d}V} = \frac{I}{\mathrm{d}V/\mathrm{d}t} = g(V) \tag{4}$$

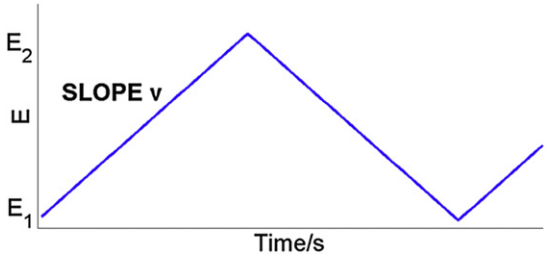


**Fig. 1.** Potential-time profiles for cyclic voltammetry.

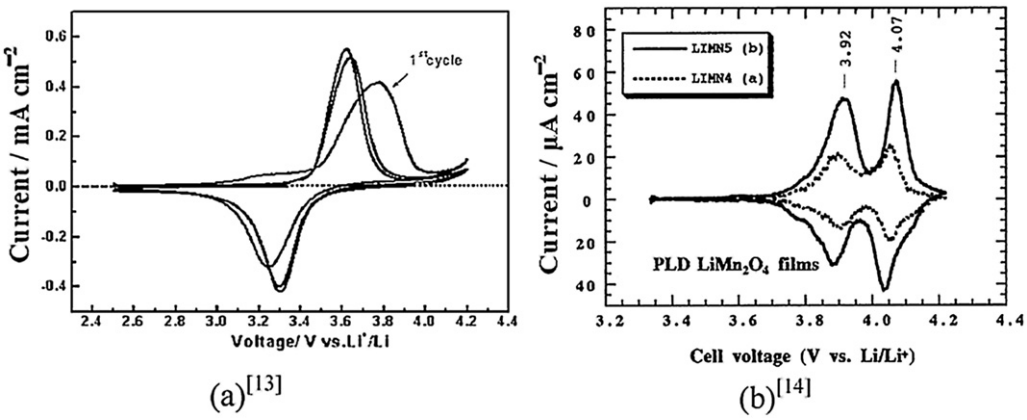


**Fig. 2.** Typical voltammograms for $LiFePO_4$(a) and $LiMn_2O_4$(b).

$$I = \frac{dV}{dt}\cdot g(V) = f_{IC-DV}(V) \tag{5}$$

### 2.2. Derivation of the equivalence of the PDF and the ICA/DVA

However, when calculating the value of $dV$, the data processing for the ICA and the DVA may encounter problems. As stated above, batteries with either a $LiFePO_4$ cathode or a $LiMn_2O_4$ cathode employ one or more voltage platforms (Fig. 3). The adjacent sampled value of voltage may be the same, when the voltage plateaus occur. As can be observed in Table 1, from 8029 s to 8055 s, the sampled voltage remains constant at 3.198 V during the $C/3$ discharge. Such a situation is quite common for our BMS and battery test bench that has a sampling resolution of 1 mV.

When $dV$ is calculated using a two-point numerical differentiation, sometimes $dV = 0$ and noise peaks can occur that affect the data processing [9]. Although such problems can be solved by a preliminary curve fitting step, an ordinary BMS may not be capable of doing this. Furthermore, the resolution of the voltage measurement may not be adequate to distinguish the voltage difference when the voltage plateaus occur during a C/D test. Even if the measurements are acceptable, the noise may be removed, it leads to a higher cost for the sampling module of the BMS.

Though curve fitting may help, the probability density function (PDF) method can provide a simpler solution. That is to say, statistical methods are applied to the C/D data of voltage. Because the C/D procedure at a low current (e.g. $C/3$) leads to approximately $3 \times 3600 = 10800$ sampling points, the statistical method is applicable. The statistical results are depicted in Fig. 4. Fig. 4(b) shows the histogram of discharge voltage (Fig. 4(a)) plotted by MATLAB®. And Fig. 4(c) is the PDF map of the voltage, including smoothing of Fig. 4(b) using *ksdensity*, a function in the Statistics Toolbox for MATLAB®.

A detailed derivation is provided below to verify the equivalence between the PDF and the ICA/DVA. For the discrete sampling system, $dV$ is replaced by $\delta V$, where $\delta V = 1$ mV. Additionally, $dQ$ is replaced by $\delta Q$, where $\delta Q = 1\ \text{s} \times I\ (\text{As})$, and $I = C/3$, as in Fig. 5.

For the derivation, assume a specific value of $V_{d,k}$, where d denotes digital and k is the index of an element in the series. First, $V_{d,k}$ complies with Eq. (6), where for charging, $V_0$ equals the voltage at the start of battery charging: e.g., 2.800 V for an LFP. Accordingly, there is a digital value $Q_{d,n}$ as given by Eq. (7), and $Q_{d,n}$ is proportional to the current $I$. In supplement, there is a difference between $V_{d,k}$ and $Q_{d,n}$: in time series, $V_d(t)$ may equals $V_d(t+1)$ when voltage plateau occurs, but $Q_d(t)$ never equals $Q_d(t+1)$.

$$V_{d,k} = V_0 + k \times \delta V (k = 0, 1, 2\ldots) \tag{6}$$

$$Q_{d,n} = Q_0 + n \times dQ = n \cdot I \cdot t\ (n = 0, 1, 2\ldots Q_0 = 0,\ \text{for charging}) \tag{7}$$

**Table 1**
Example of sampling data encountering a voltage platform.

| Time/s | ⋯ | 8028 | 8029 | ⋯ | 8054 | 8055 | 8056 | 8057 | 8058 | ⋯ |
|---|---|---|---|---|---|---|---|---|---|---|
| Volt/V | | 3.199 | 3.198 | 3.198 | 3.198 | 3.198 | 3.197 | 3.198 | 3.197 | |

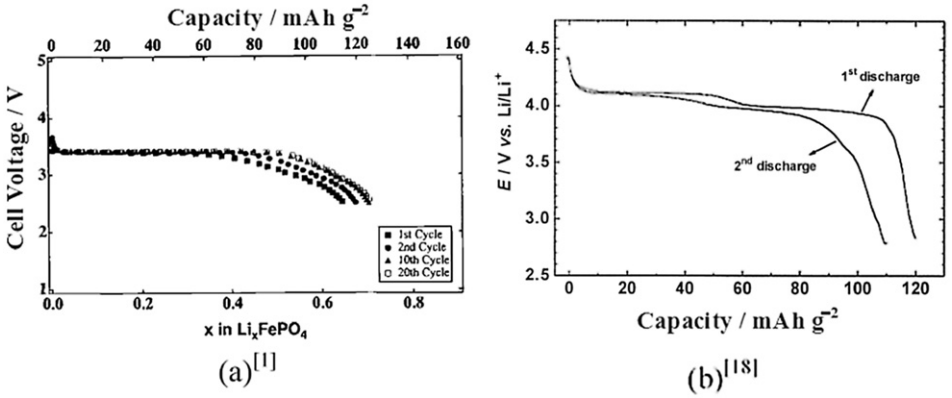


**Fig. 3.** Typical discharging curve for $LiFePO_4$(a) and $LiMn_2O_4$(b) [18].

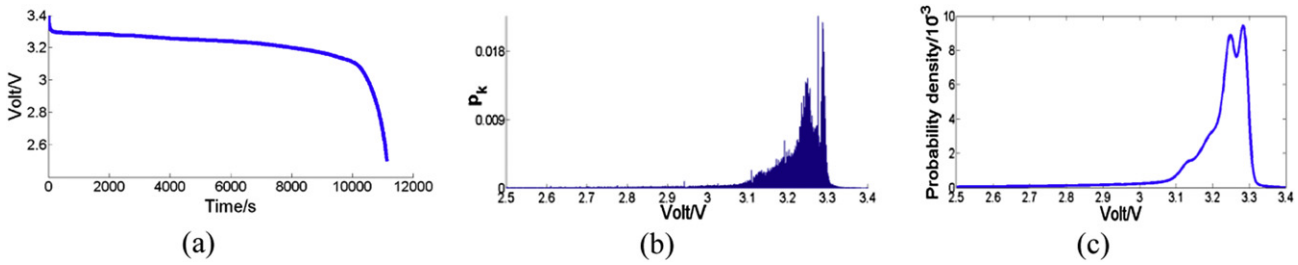


**Fig. 4.** Typical results of the PDF method.

Second, as in Eq. (3), there is $Q_a$ corresponding to $V_d$, where subscript a denotes analog, given by Eq. (8). Next, assuming that $V_a$ conforms to Eq. (9), then the corresponding value $V_d$ satisfies $V_d = V_{d,k}$. Moreover, using Eq. (8), the values of capacity $Q_{a,k}$ and $Q_{a,k+1}$ must satisfy Eq. (10) and Eq. (11).

$$Q_a = f^{-1}(V_d) \tag{8}$$

$$\text{If } V_{d,k} \le V_a < V_{d,k+1}, \text{ then } V_d = V_{d,k} \tag{9}$$

$$Q_{a,k} = f^{-1}(V_{d,k}); Q_{a,k+1} = f^{-1}(V_{d,k+1}) \tag{10}$$

$$Q_{d,l} \le Q_{a,k} < Q_{d,l+1} < Q_{d,m} \le Q_{a,k+1} < Q_{d,m+1}, \quad (m,l = 0,1,2\ldots) \tag{11}$$

Thus, when a statistical calculation is done at $V_{d,k}$, the frequency $N_k$ for $V_{d,k}$ should be $m - l + 1$ as shown in Eq. (12). In addition, considering the number of samples in the data set $L$, the probability $p_k$ of $V_{d,k}$ should be $N_k/L$, which is Eq. (13).

$$N_k = m - l + 1 \tag{12}$$

$$p_k = N_k/L \tag{13}$$

For comparison, consider the PDF and the ICA/DVA. At the point of $V_{d,k}$, the derivative $dQ/dV$ is approximated from Eq. (14). As shown by Eqs. (15) and (16), the result is approximately proportional to $N_k$ or $p_k$.

$$\left.\frac{dQ}{dV}\right|V_{d,k} = \frac{Q_{a,k+1} - Q_{a,k}}{V_{d,k+1} - V_{d,k}} = \frac{Q_{a,k+1} - Q_{a,k}}{\delta V} \tag{14}$$

$$(m-l-1)\cdot\frac{\delta Q}{\delta V} = \frac{Q_{d,m} - Q_{d,l+1}}{\delta V} < \left.\frac{dQ}{dV}\right|V_{d,k} < \frac{Q_{d,m+1} - Q_{d,l}}{\delta V} = (m-l+1)\cdot\frac{\delta Q}{\delta V} \tag{15}$$

$$\left.\frac{dQ}{dV}\right|V_{d,k} \approx (m-l+1)\cdot\frac{\delta Q}{\delta V} = N_k\cdot C_{QV} = p_k\cdot L\cdot C_{QV}, \left(C_{QV} = \frac{\delta Q}{\delta V}\right) \tag{16}$$

Because of the capacity fade due to cycling, $dQ/dV$ should be normalized by $Q_{C0}$. $Q_{C0}$ is proportional to the length of the test data $L$, as shown in Eq. (17). The normalized $dQ/dV$ remains proportional to $p_k$.

$$Q_{C0} = It \propto L \tag{17}$$

$$\frac{1}{Q_{C0}}\cdot\left.\frac{dQ}{dV}\right|V_{d,k} \propto \frac{1}{L}(m-l+1)\cdot\frac{\delta Q}{\delta V} = p_k\cdot C_{QV}, \left(C_{QV} = \frac{\delta Q}{\delta V}\right) \tag{18}$$

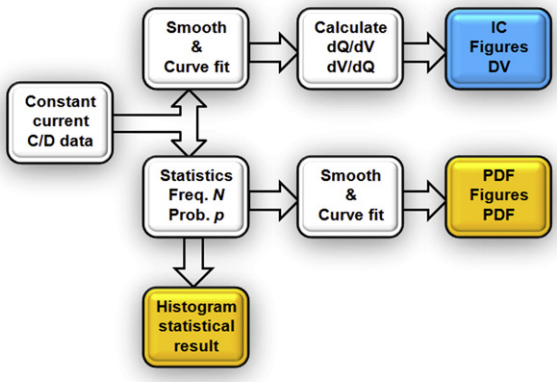


**Fig. 6.** The relationship between the PDF and the ICA/DVA.

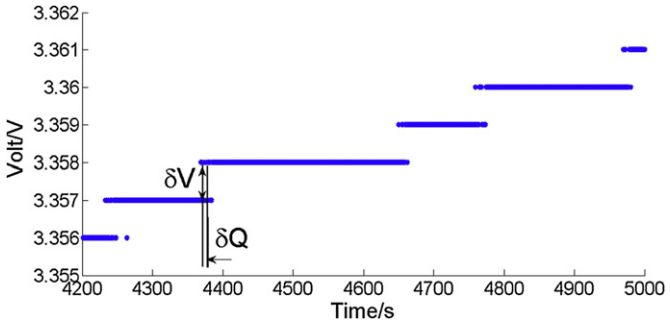


**Fig. 5.** Illustration for $\delta Q$ and $\delta V$ derived from Fig. 4(a).

**Table 2**
Specifications of the batteries.

| No. | Code | Cathode | Anode | Capacity/Ah | Test procedure | Attribute |
|---|---|---|---|---|---|---|
| 1 | Coin-F | $LiFePO_4$ | Li | $0.861 \times 10^{-3}$ | 1 | Self-made coin, cathode from F-2 |
| 2 | Coin-M | $LiMn_2O_4$ | Li | $0.817 \times 10^{-3}$ | 1 | Self-made coin, cathode from M-2 |
| 3 | F-1 | $LiFePO_4$ | C | 70 | 2 | Commercial power |
| 4 | F-2 | $LiFePO_4$ | C | 11 | 2 | Commercial power |
| 5 | M-1 | $LiMn_2O_4$ | C | 10 | 2 | Commercial power |
| 6 | M-2 | $LiMn_2O_4$ | C | 35 | 2 | Commercial power |

**Table 3**
Test profile 1 for the coin cells.

| Step no. | Step name | Duration | Current | Cycle no. |
|---|---|---|---|---|
| 1 | Rest | 60 min | | |
| 2 | Charge | | 0.1 C | |
| 3 | Discharge | | 0.1 C | |
| 4 | Rest | 60 min | | |
| 5 | Charge | | 1/3 C | |
| 6 | Discharge | | 1/3 C | |
| 7 | Cycle, step 4–6 | | | 2 |
| 8 | End | | | |

**Table 4**
Test profile 2 for the commercial batteries.

| Step no. | Step name | Duration | Condition | Cycle no. |
|---|---|---|---|---|
| 1 | Rest | 60 min | | |
| 2 | Discharge | | $I = C/3$ | |
| 3 | Rest | 60 min | | |
| 4 | Charge | | $I = C/3$ | |
| 5 | Constant voltage charge | | $V$ = upper limit | |
| 6 | Accelerating aging test | | | |
| 7 | Cycle, step 2–6 | | | Continuing |
| 8 | End | | | |

Based on the derivation above, a histogram can be drawn to illustrate the relationship between $p_k$ and $V$, as shown in Fig. 4(b). Moreover, if the probability density function is calculated using *ksdensity* in MATLAB®, the histogram is smoothed as shown in Fig. 4(c). Fig. 4(b and c) are both referred to as the results of the PDF method. Because the PDF and the ICA/DVA have the same basis, similar conclusions can be drawn when analyzing C/D data. The detailed analysis conducted using the PDF method is described in Section 4.

In conclusion, the PDF method and the ICA/DVA method have the same characteristics, as can be observed in Fig. 6.

## 3. Experiment

In this section, the details of the battery experiments are provided, and the data to be analyzed in Section 4 were acquired from these tests.

### 3.1. The test batteries

Table 2 lists the specifications of the batteries used for tests. Two coin cells were constructed, one with a $LiFePO_4$ cathode, the other with a $LiMn_2O_4$ cathode. The cathode materials of them are tailored from the electrodes of the commercial battery, F-2 and M-2, respectively. Each of the coin cells had a Li metal anode. In addition, four commercial batteries were tested. Two of them had $LiFePO_4$ cathodes and the other two had $LiMn_2O_4$ cathodes.

### 3.2. The test profiles

Two test profiles were established. The profile to test the coin cells is described in Table 3 (Pro. 1), and the profile to test the commercial batteries is described in Table 4 (Pro. 2).

For the coin cells, the PDF analysis mainly focused on the $C/3$ C/D cycle. The high/low voltage limit was 3.8/3.2 V for $LiFePO_4$ and 4.3/3.5 V for $LiMn_2O_4$.

CV tests were obtained for the coin-F and coin-M, using AUTOLAB PGSTAT302 (Metrohm, Switzerland). The scan rate for $LiFePO_4$/Li was 100 $\mu V\ s^{-1}$ and 20 $\mu V\ s^{-1}$ for $LiMn_2O_4$/Li. The scan range was 2.5–4.2 V for $LiFePO_4$/Li and 3.3–4.2 V for $LiMn_2O_4$/Li.

For the commercial batteries, the PDF analysis mainly focused on the cycle life. The test profile is shown in Table 4. Accelerated aging was used to simulate the aging process of the battery. When the PDF method is employed to analyze the data, the step of the constant voltage charging is excluded.

## 4. PDF results and discussions

In this section, the results using the PDF method are provided, and the function of the PDF method is explained.

### 4.1. Test results for the coin cells

For the coin cells, the $C/3$ C/D cycle is analyzed using the PDF method. The results are compared with those from the CV tests of the identical cells. The C/D curve and the PDF graph of $LiFePO_4$/Li cell and $LiMn_2O_4$/Li cell are shown in Figs. 7 and 8, respectively.

The peak number of the PDF curves are quite similar to that of the CV curves (Figs. 2, 7 and 8). That is a verification for the

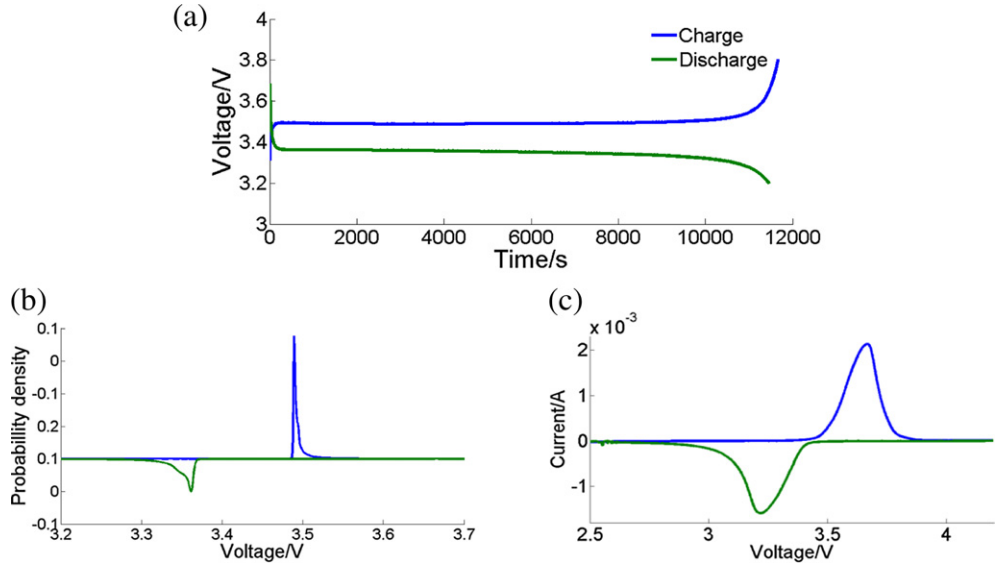


**Fig. 7.** 1/3C cycle data of the $LiFePO_4$/Li, (a) C/D curve, (b) PDF curve, (c) CV curve.

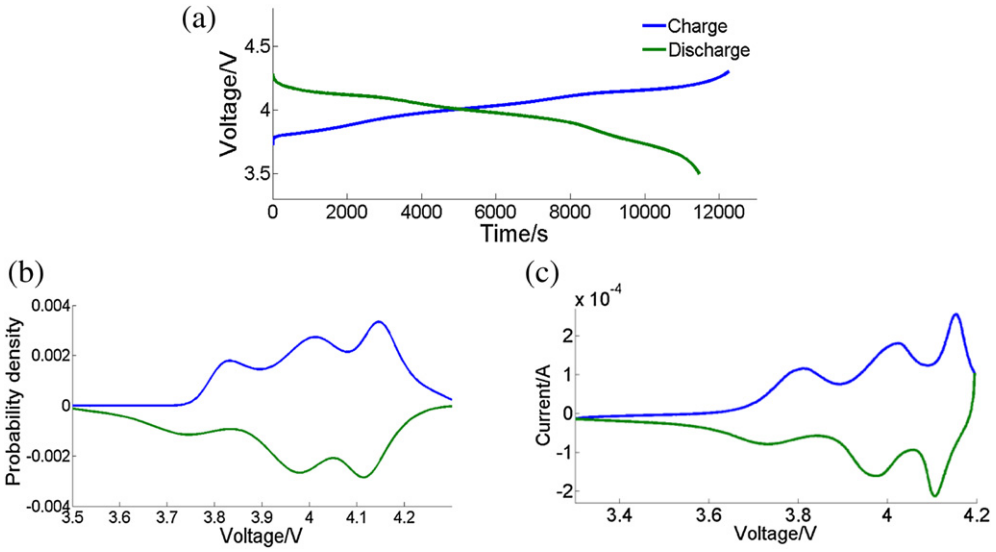


**Fig. 8.** 1/3C cycle data of the LiMn2O4/Li, (a) C/D curve, (b) PDF curve, (c) CV curve.

derivation in Sections 3.1 and 3.2. The locations of the peaks are compared in Table 5 and Table 6. For $LiFePO_4$, the CV and the PDF both have a peak for charging and the other peak for discharging. While the location of the peak from the PDF method for $LiFePO_4$ is a little different from that of the CV. That may be due to the polarization of the cathode material. Nevertheless, these peaks comply with the process of lithium intercalation and de-intercalation. For $LiMn_2O_4$ the locations of the peaks from the PDF method are quite similar to those from the CV. These peaks are all representative of the lithium intercalation and de-intercalation process.

### 4.2. Cycle life test of the commercial batteries

In this section, the experimental data are analyzed to verify that the PDF method can be used in cycle life tests for batteries. The C/D cycle was performed as listed in Table 4. Fig. 9 shows the C/D data of the F-1, F-2, M-1 and M-2 batteries, respectively. Figs. 10–13 show the PDF results for the 4 types of batteries. These results show the C/D data (Fig. 9) at different cycle numbers. For F-1, F-2 and M-1, the cycle numbers selected are 0, 150, 300 and 450, but for M-2, because the life of M-2 ended at the 240th cycle, the cycle numbers selected are 0, 60, 150 and 210. In the legend, the "C" suffix denotes "charging" and "D" denotes "discharging". The integration areas of the PDF curves are all 1.

Fig. 10(b and c) are magnified sub-figures within the rectangles in Fig. 10(a). The PDF results for F-1, F-2 and M-1 are all shown in three sub-figures. The changing trends of the peak magnitude with increasing cycle number are indicated by arrows in those magnified figures. The changing trends for M-2 are visible without magnification.

Considering the PDF results for $LiFePO_4$, it can be clearly observed that in sub-figures (b) and (c) of both Figs. 10 and 11, a similar regularity occurs around the peak. The arrows mark the changing trend. To be specific, the magnitude of the second peak (locating at approximately 3.4 V) decreases as the cycle number increases, and the capacity fades. In other words, the second voltage plateau is shortening as the battery is aging. Importantly, this phenomenon has been discovered in our recent researches on battery longevity.

The PDF results for $LiMn_2O_4$ are discussed next. First, for the M-1 battery, the valley between the two peaks rises as the cycle number increases. That means that when the battery is aging, the two voltage platforms for the $LiMn_2O_4$ battery are getting closer and closer, and tends to share a similar voltage slope. However, for the M-2 battery, the PDF curve is moving as indicated by the arrows as the battery ages.

### 4.3. Statistics and algorithm

As observed in Section 4.2, the probability magnitude at and around the peak displays a consistent regularity as the capacity fades. As a result, if the frequency within a specific threshold is integrated, the integration should have the same trend as that of the peak magnitude. To be specific, the integration threshold for the $LiFePO_4$ batteries, F-1 and F-2, is 3.27/3.26–3.30 V (for discharging) and 3.38–4.42 V (for charging), as shown in Table 7. The second peak locates at approximately 3.28 V (for discharging) and 3.40 V (for charging), as shown in Fig. 10(b and c). Thresholds for $LiMn_2O_4$ are also listed in Table 7. In Table 7, the values of $N$, the integrated frequencies of the voltage within the integration thresholds are listed, too. Note that when $N$ is divided by the data length $L$ or the C/D time, the result is $p$. The $p$ and data length (or the total C/D time)

**Table 5**
Comparison of the peak positions for $LiFePO_4$.

| Reference | Cathode/anode | Charge/discharge | Peak separation/V | Method |
|---|---|---|---|---|
| | | Peak position/V | | |
| This paper | $LiFePO_4$/Li | 3.49/3.36 | 0.13 | PDF |
| This paper | $LiFePO_4$/Li | 3.67/3.22 | 0.45 | CV |
| [13] | $LiFePO_4$/Li | 3.80/3.25 | 0.55 | CV |
| [19] | $LiFePO_4$/Li | 4.08/2.88 | 1.20 | CV |

**Table 6**
Comparison of the peak position for $LiMn_2O_4$.

| Reference | Cathode | Charge/discharge | | | Peak separation/V | Method |
|---|---|---|---|---|---|---|
| | | Peak1/V | Peak2/V | Peak3/V | | |
| This paper | $LiMn_2O_4$/Li | 3.83/3.75 | 4.01/3.98 | 4.15/4.11 | (0.18,0.13)/(0.14,0.13) | PDF |
| This paper | $LiMn_2O_4$/Li | 3.81/3.73 | 4.03/3.97 | 4.15/4.11 | (0.18,0.12)/(0.14,0.14) | CV |
| [14] | $LiMn_2O_4$/Li | 3.92/3.88 | 4.07/4.03 | – | 0.15/0.15 | CV |
| [17] | $LiMn_2O_4$/Li | 4.10/3.90 | 4.25/4.05 | – | 0.15/0.15 | CV |

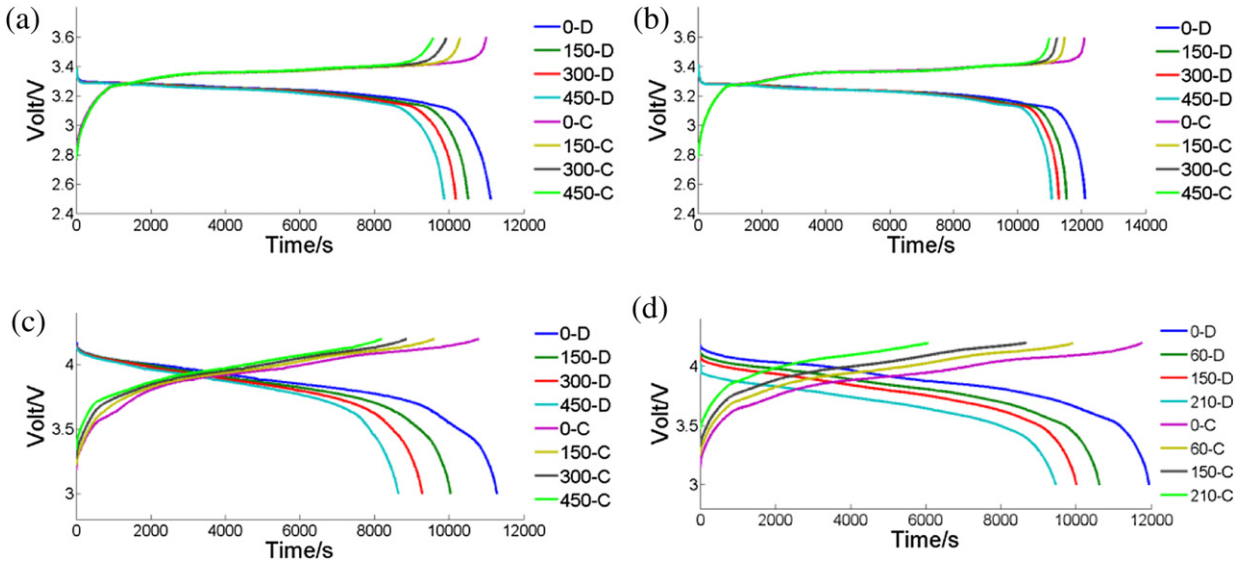


**Fig. 9.** C/D curves for battery F-1 (a), F-2 (b), M-1 (c), M-2 (d).

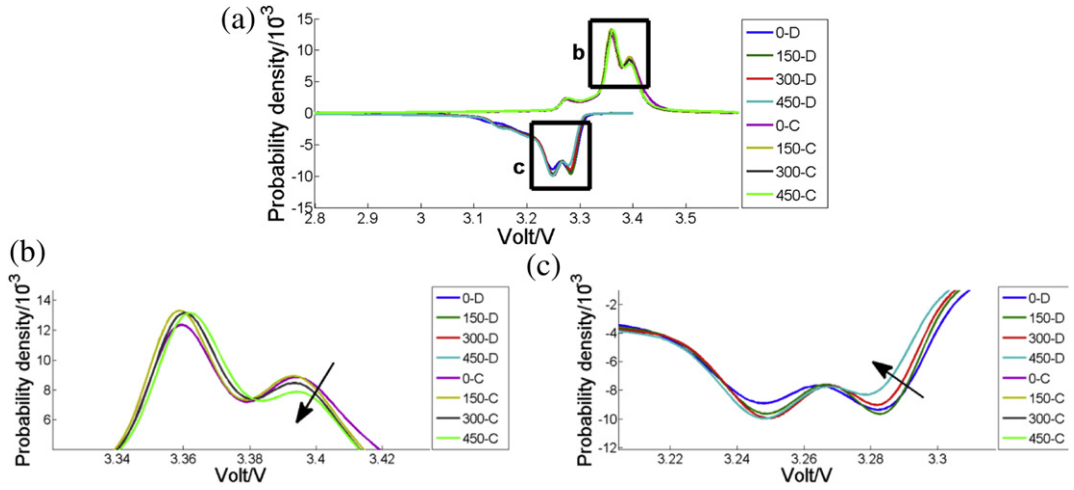


**Fig. 10.** PDF result for the F-1 battery.

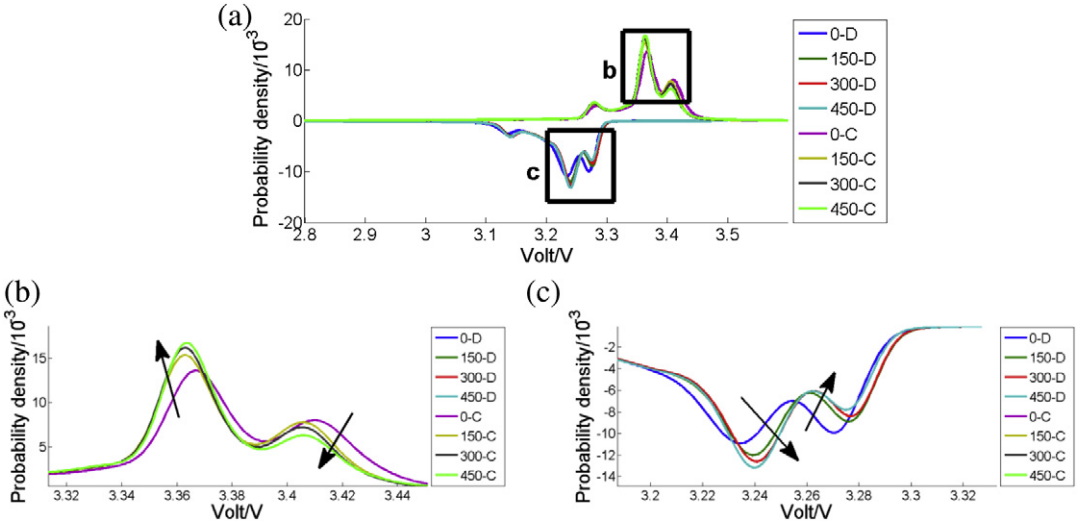


**Fig. 11.** PDF result for the F-2 battery.

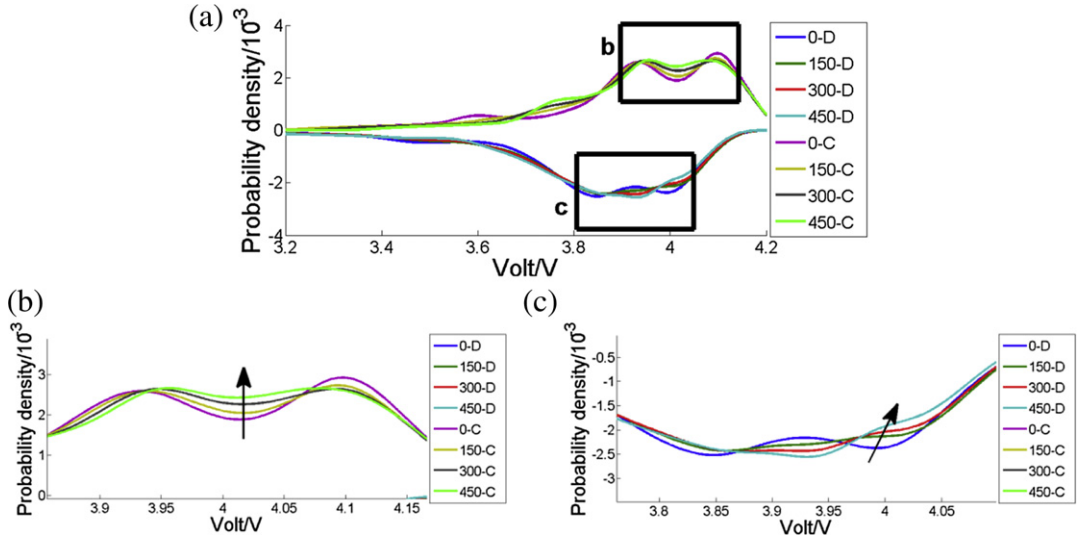


**Fig. 12.** PDF result for the M-1 battery.

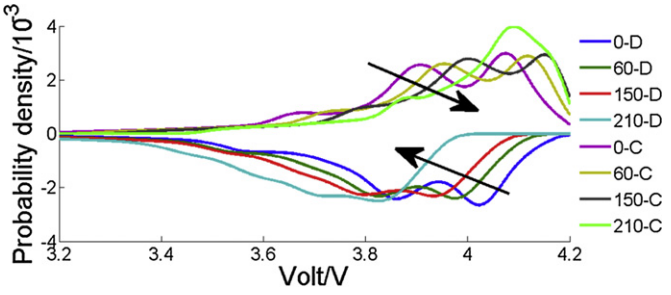


**Fig. 13.** PDF result for the M-2 battery.

are shown in Fig. 14. Because the C/D tests employ the constant current $C/3$, the total C/D time is proportional to the battery capacity.

Based upon the discussion above, the PDF curves reveal the relationship between the statistics and the battery longevity. So a possible algorithm using the PDF results to evaluate the SOH of battery is proposed (see Fig. 15). First, in the laboratory, a constant current, e.g., $C/3$, can be chosen to perform battery aging test. Then, using the PDF method, the changing trend of the curve peak corresponding to the battery aging can be synthesized. A characteristic peak-neighborhood voltage range, e.g. 3.38–3.42 V, for the $LiFePO_4$ charging, can be determined. A map of statistical integration values and the corresponding capacities (total C/D time) can be developed.

Based on the laboratory test, a possible online evaluation of SOH can be performed. Rather than conducting a complete C/D test, a partial C/D test can be conducted at the same constant current, e.g., $C/3$. Naturally, the partial C/D process should cover the threshold, e.g. 3.38–3.42 V for charging. Next, a count of the points within the voltage threshold is performed. For example, for a $LiFePO_4$ battery, if the frequency of the voltage within 3.38–3.42 V during partial charging is $N_c = 2590$, between 2386 and 2621 (in bold) in Table 7. From Table 7, the interpolated value of data length is 9884. The data length $L$ of the first cycle equals 10998. Therefore, the evaluated relative charging capacity should be 9884/10998 = 90%. A similar process can be conducted to obtain the relative discharging capacity for the battery.

### 4.4. Algorithm verification and discussion

To verify the algorithm, cycle data for the F-1 battery were randomly selected. The frequency during partial charging/

**Table 7**
Statistical integrated values of $N$ and $p$ for the 4 types of commercial batteries.

| Battery code | Discharge | | | | | Charge | | | | |
|---|---|---|---|---|---|---|---|---|---|---|
| | Cycle | Integration range/V | Data length $L$ | $N$ | $p$ | Cycle | Integration range/V | Data length $L$ | $N$ | $P$ |
| F-1 | 0 | 3.27–3.30 | 11,113 | 2894 | 0.260 | 0 | 3.38–3.42 | 10,998 | 3134 | 0.285 |
| | 150 | | 10,508 | 2669 | 0.254 | 150 | | 10,298 | 2881 | 0.280 |
| | 300 | | 10,180 | 2370 | 0.233 | 300 | | 9931 | **2621** | **0.264** |
| | 450 | | 9866 | 2011 | 0.204 | 450 | | 9574 | **2386** | **0.249** |
| F-2 | 0 | 3.26–3.30 | 12,106 | 2860 | 0.236 | 0 | 3.38–3.42 | 12,091 | 3243 | 0.268 |
| | 150 | | 11,527 | 2620 | 0.227 | 150 | | 11,471 | 2896 | 0.252 |
| | 300 | | 11,289 | 2408 | 0.213 | 300 | | 11,230 | 2622 | 0.233 |
| | 450 | | 11,063 | 2097 | 0.190 | 450 | | 10,999 | 2344 | 0.213 |
| M-1 | 0 | 3.95–4.05 | 11,280 | 2605 | 0.231 | 0 | 3.95–4.05 | 10,806 | 2116 | 0.196 |
| | 150 | | 10,040 | 2167 | 0.216 | 150 | | 9609 | 2052 | 0.214 |
| | 300 | | 9280 | 1961 | 0.211 | 300 | | 8862 | 2087 | 0.235 |
| | 450 | | 8637 | 1743 | 0.202 | 450 | | 8197 | 2063 | 0.252 |
| M-2 | 0 | 3.95–4.05 | 11,946 | 2969 | 0.249 | 0 | 3.80–3.90 | 11,757 | 2088 | 0.178 |
| | 60 | | 10,619 | 2360 | 0.222 | 60 | | 9921 | 1225 | 0.123 |
| | 150 | | 10,006 | 1511 | 0.151 | 150 | | 8677 | 971 | 0.112 |
| | 210 | | 9456 | 11 | 0.001 | 210 | | 6062 | 628 | 0.104 |

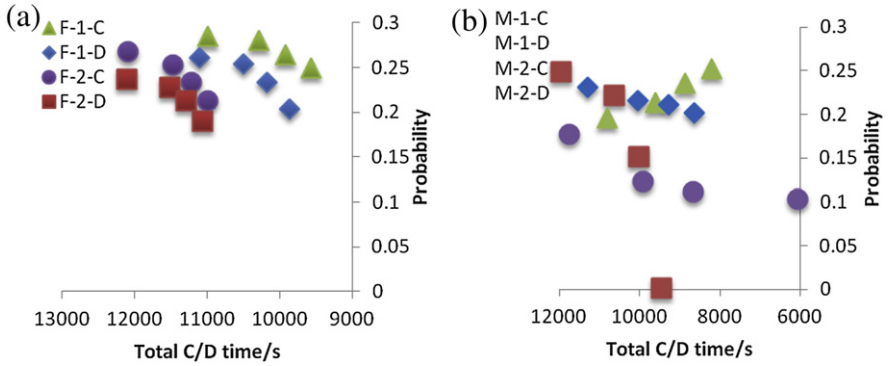


**Fig. 14.** Relationship between the total probability within the threshold and the total C/D time.

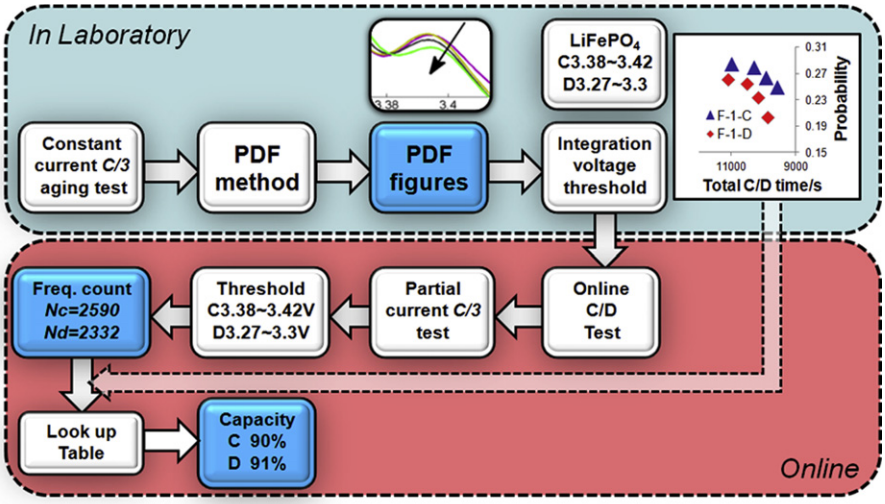


**Fig. 15.** A possible algorithm to evaluate the battery SOH online by PDF method.

discharging was collected, and the frequency $N$ was transformed into the evaluated capacity (Table 8). Compared with the actual capacity, the evaluation error is within 2% most of the time.

In addition, we wish to discuss the advantages of the PDF method here. For online applications to evaluate the SOH of the battery, the ICA/DVA method requires curve fitting first and then the peak value must be determined and compared with an embedded table. However, in the PDF method, only a scan through the complete data set is required. Letting the total number of data points be $n$, the complexity of both algorithms is $O(n)$, but for the ICA/DVA method, the number of calculations should be much larger than $n$, whereas that of the PDF method should be less than $n$.

**Table 8**
Evaluation error of the PDF algorithm.

| Data number | | 1 | 2 | 3 | 4 | 5 |
|---|---|---|---|---|---|---|
| Charge | Frequency $N$ | 2931 | 2661 | 2597 | 2565 | 2493 |
| | Evaluated capacity/% | 94.9 | 90.8 | 90.0 | 89.5 | 88.5 |
| | Actual capacity/% | 94.6 | 92.3 | 91.6 | 89.6 | 89.1 |
| | Evaluation error/% | 0.3 | −1.5 | −1.6 | −0.1 | −0.6 |
| Discharge | Frequency $N$ | 2822 | 2658 | 2631 | 2242 | 2240 |
| | Evaluated capacity/% | 98.3 | 94.4 | 94.2 | 90.6 | 90.6 |
| | Actual capacity/% | 95.1 | 93.1 | 92.3 | 91.1 | 90.6 |
| | Evaluation error/% | 3.2 | 1.3 | 1.9 | −0.5 | 0.0 |

The PDF method may be regarded as an extension of the ICA/DVA method, because we have verified that the PDF method and the ICA/DVA method have the same basis. The PDF method takes a substantial step in allowing the ICA/DVA method to be applied in an online BMS. The PDF algorithm has privilege in online evaluation of SOH. For one thing, the PDF algorithm saves time due to its partial C/D test. For another, no curve fitting is required and only easy counting work is essential for the BMS.

## 5. Conclusion

This paper introduces a new method, the PDF method, to analyze the C/D data of electric storage batteries. A comparison of the PDF, the CV and the ICA/DVA method is given. Importantly, the verification of the equivalent basis of the PDF and the ICA/DVA is derived. Given that the PDF and the ICA/DVA have the same basis, the results when analyzing battery C/D data are quite similar. In addition, $LiFePO_4$ and $LiMn_2O_4$ batteries are employed to test the PDF method. Actual data show that the PDF results and the CV results have the same shape. The PDF method is introduced to analyze the aging behavior of sample batteries. The specific magnitude of the PDF peak decreases as the battery capacity fades. Employing the regularity of the peak fading with battery aging, an algorithm is proposed to evaluate the SOH online using a partial C/D test. The algorithm is verified by experimental data. And we

believe the PDF method takes a substantial step in allowing the ICA/DVA method to be applied in online SOH evaluation.

The PDF method origins from classical probability theory. Recently, our group are attempting to utilize the PDF method in data processing, especially for the signals acquired from battery operating conditions. When we followed the method proposed in Refs. [5,7,9], we initially encountered a problem to calculate $dV$. The sampling resolution of our instrument restricted the process, when we followed the instruction to perform the curve fitting. So we turned to the PDF method to obtain a solution more easily, as we did in Ref. [12], although a partial curve fitting is feasible for the pre-process of the ICA/DVA method. Furthermore, we found that the PDF results are quite similar to those of the ICA/DVA. We were trying to verify the equivalence of the PDF method and the ICA/DVA method and finally we succeeded.

## Acknowledgment

This work is funded by the MOST (Ministry of Science and Technology) of China under the contract of No. 2010DFA72760 and also by the NSFC (National Natural Science Foundation) of China under contract No. 61004075.

The authors would like to thank Prof. Jing Sun and Prof. Huei Peng from the University of Michigan for advice. Their recent work on the SVR method used in the ICA/DVA analysis also broadens the vision of the SOH evaluation research. We would also like to thank Dr. Jian Gao, Mr. Hao Wang and Mr. Jiang Cao from the Institute of Nuclear and New Energy Technology, Tsinghua University, who assisted us in conducting the CV tests.

## References

[1] A.K. Padhi, K.S. Nanjundaswamy, J.B. Goodenough, J. Electrochem. Soc. 144 (1997) 1188–1194.
[2] S. Ma, H. Noguchi, M. Yoshio, J. Power Sources 97–98 (2001) 385–388.
[3] Southampton electrochemistry group, Instrumental Methods in Electrochemistry, Ellis Horwood, London, 1985, pp. 178–227.
[4] C.H. Hamann, A. Hamnett, W. Vielstich (Eds.), Electrochemistry, second ed., Chemical Industry Press, Beijing, 2010, pp. 197–208 (Interpreted in Chinese).
[5] J. Groot, State-of-Health Estimation of Li-ion Batteries: Cycle Life Test Methods, Göteborg, Sweden, 2012.
[6] E. Meissner, G. Richter, J. Power Sources 116 (2003) 79–98.
[7] M. Dubarry, B.Y. Liaw, J. Power Sources 194 (2009) 541–549.
[8] I. Bloom, A.N. Jansen, D.P. Abraham, et al., J. Power Sources 139 (2005) 295–303.
[9] J.P. Christophersen, S.R. Shaw, J. Power Sources 195 (2010) 1225–1234.
[10] F. Huet, J. Power Sources 70 (1998) 59–69.
[11] P. Singh, S. Kaneria, J. Broadhead, X. Wang, J. Burdick, in: INTELEC 26th Annual International Telecommunications Energy Conference, Chicago, IL, USA, 2004, pp. 524–531.
[12] X. Feng, J. Li, L. Lu, J. Hua, L. Xu, M. Ouyang, J. Power Sources 209 (2012) 30–39.
[13] X. Liao, Z. Ma, L. Wang, et al., Electrochem. Solid-State Lett. 7 (2004) 522–525.
[14] C. Julien, E. Haro-Poniatowski, M.A. Camacho-Lopez, et al., Mater. Sci. Eng. B72 (2000) 36–46.
[15] PNGV Battery Test Manual, 2001.
[16] Battery Test Manual for Plug-in Hybrid Electric Vehicles, Idaho National Laboratory, 2008.
[17] Z. Li, L. Lu, M. Ouyang, Y. Xiao, J. Power Sources 196 (2011) 9757–9766.
[18] L.C. Ferracin, F.A. Amaral, N. Bocch, Solid State Ionics 130 (2000) 215–220.
[19] H. Liu, C. Li, H. Zhang, et al., J. Power Sources 159 (2006) 717–720.